



Site-specific climatic signals in stable isotope records from Swedish pine forests

Jan Esper¹ · Steffen Holzkämper² · Ulf Büntgen^{3,4,5} · Bernd Schöne⁶ · Frank Keppler⁷ · Claudia Hartl¹ · Scott St. George⁸ · Dana F. C. Riechelmann⁶ · Kerstin Treydte⁴

Received: 2 November 2017 / Accepted: 19 February 2018 / Published online: 23 February 2018
© Springer-Verlag GmbH Germany, part of Springer Nature 2018

Abstract

Key message *Pinus sylvestris* tree-ring $\delta^{13}\text{C}$ and $\delta^{18}\text{O}$ records from locally moist sites in central and northern Sweden contain consistently stronger climate signals than their dry site counterparts.

Abstract We produced twentieth century stable isotope data from *Pinus sylvestris* trees near lakeshores and inland sites in northern Sweden (near Kiruna) and central Sweden (near Stockholm) to evaluate the influence of changing microsite conditions on the climate sensitivity of tree-ring $\delta^{13}\text{C}$ and $\delta^{18}\text{O}$. The data reveal a latitudinal trend towards lower C and O isotope values near the Arctic tree line (-0.8‰ for $\delta^{13}\text{C}$ and -2.4‰ for $\delta^{18}\text{O}$ relative to central Sweden) reflecting widely recognized atmospheric changes. At the microsite scale, $\delta^{13}\text{C}$ decreases from the dry inland to the moist lakeshore sites (-0.7‰ in Kiruna and -1.2‰ in Stockholm), evidence of the importance of groundwater access to this proxy. While all isotope records from northern and central Sweden correlate significantly against temperature, precipitation, cloud cover and/or drought data, climate signals in the records from moist microsites are consistently stronger, which emphasizes the importance of site selection when producing stable isotope chronologies. Overall strongest correlations are found with summer temperature, except for $\delta^{18}\text{O}$ from Stockholm correlating best with instrumental drought indices. These findings are complemented by significant positive correlations with temperature-sensitive ring width data in Kiruna, and inverse (or absent) correlations with precipitation-sensitive ring width data in Stockholm. A conclusive differentiation between leading and co-varying forcings is challenging based on only the calibration against often defective instrumental climate data, and would require an improved understanding of the physiological processes that control isotope fractionation at varying microsites and joined application of forward modelling.

Keywords $\delta^{13}\text{C}$ · $\delta^{18}\text{O}$ · *Pinus sylvestris* L. · Microsite · Dendrochronology · Sweden

Introduction

Stable carbon and oxygen isotope ratios ($\delta^{13}\text{C}$ and $\delta^{18}\text{O}$ values) are valuable proxies for reconstructing long-term climatic changes at annual resolution (Leavitt 2010).

Communicated by A. Gessler.

✉ Jan Esper
esper@uni-mainz.de

¹ Department of Geography, Johannes Gutenberg University, Mainz, Germany

² Department of Physical Geography, Stockholm University, Stockholm, Sweden

³ Department of Geography, University of Cambridge, Cambridge, UK

⁴ Swiss Federal Research Institute WSL, Birmensdorf, Switzerland

⁵ CzechGlobe Research Institute CAS and Masaryk University, Brno, Czech Republic

⁶ Institute of Geosciences, Johannes Gutenberg University, Mainz, Germany

⁷ Institute of Earth Sciences, Ruprecht-Karls University, Heidelberg, Germany

⁸ Department of Geography, Environment and Society, University of Minnesota, Minneapolis, USA

Compared to classical tree-ring width (TRW) and maximum latewood density data (MXD), which predominantly record temperature changes in cold environments (Esper et al. 2014; Luterbacher et al. 2016; Wilson et al. 2016) and hydroclimatic changes in dry environments (Cook et al. 2015; Esper et al. 2007; Tejedor et al. 2017), climate signals in stable isotopes appear to be less dependent on the ecoclimatic settings of the sampled trees (Esper et al. 2016; Frank et al. 2015; Gagen et al. 2004; Saurer et al. 2008; Treydte et al. 2007). This independency enables the use of tree-ring stable isotope records from lowland, non-boundary environments, where classical tree-ring parameters typically fail to record significant climate signals (Cernusak and English 2015; Friedrichs et al. 2008; Hartl-Meier et al. 2015) to assess long-term climatic changes at annual resolution (overview in Treydte et al. 2007, 2014).

In their analysis of a network of 23 $\delta^{13}\text{C}$ chronologies from Europe, Frank et al. (2015) showed that the maximum climatic response exhibited by that proxy encompasses a broad range of climatic parameters including relative humidity, potential evapotranspiration, maximum temperature, vapor pressure deficit and precipitation during different months and seasons during the year of ring formation. Formal reconstructions based on $\delta^{13}\text{C}$ include estimates of summer temperature variability in Central Asia (Treydte et al. 2009), winter-to-spring temperature in Turkey (Heinrich et al. 2013), summer drought in the European Alps (Kress et al. 2010), and river flow in west Siberia (Waterhouse et al. 2000). The climate sensitivity of tree-ring $\delta^{18}\text{O}$ is typically (but not always) slightly weaker compared to $\delta^{13}\text{C}$, and includes precipitation, drought and humidity signals as mechanistic drivers in addition to widely recognized temperature signals (Saurer et al. 2008; Treydte et al. 2007). Formal reconstructions based on $\delta^{18}\text{O}$ include estimates of annual precipitation in the Karakorum mountains (Treydte et al. 2006), May–August precipitation in northwest China (Liu et al. 2008) and southern England (Rinne et al. 2013), the summer standardized precipitation evapotranspiration index (SPEI) in western France (Labuhn et al. 2016), and April–July minimum temperatures in northwest Canada (Porter et al. 2014). Saurer et al. (2008) suggested the combination of tree-ring $\delta^{13}\text{C}$ and $\delta^{18}\text{O}$ may enhance the common climatic signals, an approach that was successfully carried out in northeast Canada to reconstruct summer maximum temperatures (Bégin et al. 2015).

In northern Europe, Scots pine (*Pinus sylvestris* L.) is the most common tree species and has been used in several stable isotope studies. Seftigen et al. (2011) analyzed $\delta^{13}\text{C}$ and $\delta^{18}\text{O}$ from sites in the Scandinavian mountains, and reported positive correlations with warm season temperatures, and reversed but weaker associations with precipitation. Similarly, Hiltunen et al. (2009) found July temperature signals in $\delta^{13}\text{C}$ (stronger) and $\delta^{18}\text{O}$ (weaker) in northern and

eastern Finland, as well as July precipitation signals in $\delta^{18}\text{O}$ of eastern Finland. More recently, $\delta^{13}\text{C}$ chronologies from Scandinavian pine sites were used to reconstruct sunshine hour (Loader et al. 2013) and cloud cover changes (Gagen et al. 2011). In all these assessments, the covariance among temperature, precipitation, drought indices, cloud cover and sunshine hour data was recognized as a complicating data property that makes it difficult to differentiate between directly environmental forcing and their co-variates (Frank et al. 2015).

$\delta^{13}\text{C}$ and $\delta^{18}\text{O}$ interseries correlations and climatic signals were shown to be particularly strong in the high-frequency, inter-annual domain (Konter et al. 2014). The proxies are good estimators for the reconstruction of extreme events (Treydte et al. 2001; Kress et al. 2009), but typically express less coherent lower frequency trends (Treydte et al. 2007). Work on the preservation of low frequency variance in tree-ring $\delta^{13}\text{C}$ and $\delta^{18}\text{O}$ of *Pinus uncinata* showed that both parameters contain biological age trends beyond the widely recognized juvenile effects over the first 20–30 years (Esper et al. 2010). This finding was recently confirmed for $\delta^{13}\text{C}$ using a large compilation of modern tree and sub-fossil *Pinus sylvestris* samples from Finland (Helama et al. 2015), questioning the application of such data to reconstruct low frequency climate variability (Esper et al. 2015a).

Tree-ring stable isotopes reflect the plant physiological response to climate and other environmental variables (Gessler et al. 2014; Zeng et al. 2017). $\delta^{13}\text{C}$ depends on factors affecting the photosynthetic uptake of CO_2 and is primarily controlled by stomatal conductance and the rate of carboxylation during photosynthesis (Farquhar et al. 1989). Warm and dry conditions typically reduce stomatal conductance and discrimination against ^{13}C , thus producing higher $\delta^{13}\text{C}$ values (Leavitt and Long 1989; Saurer et al. 1995). In light-limited habitats, however, carbon isotope fractionation is dominated by photo-assimilation, and high $\delta^{13}\text{C}$ values may primarily be associated with high photosynthetic activity in warm and sunny conditions (Loader et al. 2013).

Tree-ring $\delta^{18}\text{O}$ integrates the stomatal response to atmospheric vapour pressure deficit and related climate variables, such as temperature and relative humidity, via leaf water ^{18}O enrichment. Transpiration also regulates source water uptake by the roots (Barbour 2007; Roden and Ehleringer 1999), which typically originates from precipitation carrying a specific atmospheric $\delta^{18}\text{O}$ signal controlled by air mass temperature (Dansgaard 1964; Rozanski et al. 1992). This precipitation signal can be mitigated, lagged or even masked, depending on the temporal variation of the amount and isotopic composition of infiltrated water (Treydte et al. 2014), the evaporative enrichment of soil water, and the influence of ground water (Ehleringer and Dawson 1992). High soil water availability in correspondence with warm and dry conditions enhances evaporative processes at the leaf level (Darling and

Talbot 2003), which may lead to high $\delta^{18}\text{O}$ tree-ring values and partly be modified by post-photosynthetic biochemical fractionation processes (Gessler et al. 2014).

Considering these specific sensitivities, and by employing a network of locally moist and dry *Pinus sylvestris* sites in central and northern Sweden, we address the following hypotheses:

(H1) Tree-ring $\delta^{13}\text{C}$ and $\delta^{18}\text{O}$ values are lower in the colder environment of northern Sweden due to reduced photosynthesis and enzymatic fractionation ($\delta^{13}\text{C}$), relatively low transpiration and temperature effects on source water isotope fractionation ($\delta^{18}\text{O}$).

(H2) At both sites, $\delta^{13}\text{C}$ and $\delta^{18}\text{O}$ values are lower in lake-shore trees due to higher soil moisture and stomatal conductance in dry periods ($\delta^{13}\text{C}$) and unhindered access to depleted groundwater ($\delta^{18}\text{O}$).

(H3) $\delta^{13}\text{C}$ and $\delta^{18}\text{O}$ records from locally moist sites contain stronger climate signals because of increased metabolic activity and hence, isotope fractionation being more closely controlled by atmospheric weather processes. The signals are stronger in the warmer Stockholm region with larger implications of groundwater access, relative to Kiruna.

In this paper, we describe the microsite sampling scheme in central and northern Sweden, the procedures of tree-ring $\delta^{18}\text{O}$ and $\delta^{13}\text{C}$ measurement, and the statistical methods used to treat stable isotope data and compare these with instrumental climate data. We produce maps showing the spatial patterns of correlation between stable isotope and climate variables, and discuss differences in climate signals with particular focus on microsite effects. $\delta^{18}\text{O}$ and $\delta^{13}\text{C}$ chronologies are compared with TRW chronologies to support the interpretation of signal differences between locally moist and dry sites.

Materials and methods

The *Pinus sylvestris* sampling sites are located near Kiruna (hereafter, “Kir”) at 68°N and ~1000 km north of the Stockholm (“Sto”) site at 59°N (Fig. 1). Kir and Sto are underlain by a Quaternary moraine including granite blocks of up to 1 m in size. The loose substrate is 0–25 cm thick and the soil type is a sandy podsol covered by a thin (<3 cm) litter layer. Both sites are situated in the rain shadow of the Scandes, where summer precipitation approaches only 200 mm, but temperatures are 7–9 °C colder at the Arctic tree line in Kir compared to Sto (Table 1). The temperature difference affects both evaporative demand (Farquhar and Roderick 2007) and species composition, so that Kir is composed of

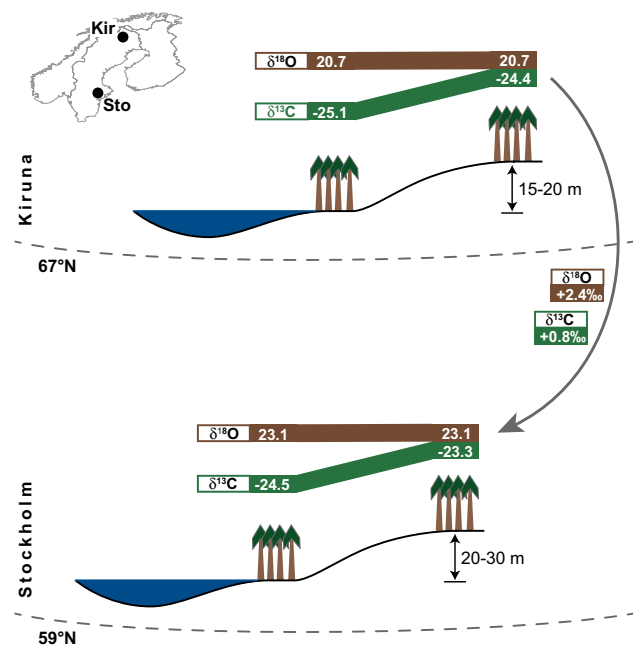


Fig. 1 Tree-ring stable isotope setup in northern (Kir) and central (Sto) Sweden. In each region, four *Pinus sylvestris* trees were sampled in locally moist (at lakeshore) and dry (several decameters inland) microsities. Values are the mean carbon (green) and oxygen isotope ratios (brown) of four trees in each microsite, as well as the difference between Kir and Sto. Standard deviations range from 0.18 (Kir-D) to 0.65 (Sto-D) for $\delta^{18}\text{O}$, and from 0.09 (Kir-M) to 0.46 (Sto-M) for $\delta^{13}\text{C}$

Table 1 Kiruna and Stockholm sampling site information

	Kir	Sto
Location	12 km NE Kiruna	11 km N Stockholm
Lat./Lon.	67.95°N, 20.03°E	59.44°N, 18.00°E
Annual temp.	-2.2 °C	7.0 °C
Summer temp.	10.0 °C	16.6 °C
Annual precip.	500 mm	560 mm
Summer precip.	200 mm	190 mm
Vegetation period	120 days	180 days

a monotonic pine forest, whereas Sto hosts a mixed forest including *Picea abies*, *Quercus robur*, *Fagus sylvatica*, and *Pinus sylvestris*. The vegetation period in Kir is 60 days shorter compared to Sto (Swedish Meteorological and Hydrological Institute, SMHI), but seasonal daylight variations are much more accentuated in northern than central Sweden. The distances between trees range from 7 to 10 m in Sto and from 3 to 10 m in Kir, and the hydroclimatic conditions during the vegetation period are classified as “weakly humid” in Kir (positive water balance of 0 to +50 mm) and “dry” in Sto (negative water balance of -50 to 0 mm; Swedish University of Agricultural Sciences).

At both sites, Kir and Sto, we used 5-mm increment borers to sample 40 pine trees growing in moist conditions within 5 m to the lakeshore (Kir-M and Sto-M) and several tens of meters inland in locally dry conditions considering all age classes in pre-defined plots (Kir-D and Sto-D; D uthorn et al. 2015, 2016). The dry microsites are located 15–30 m upslope (Kir microsites in 450 and 465 m, Sto microsites in 20 and 50 m a.s.l.) where tree roots are detached from lake filtration and phreatic water (Fig. 1). This change also impacts ground vegetation as Kir-M includes 90% bryophytes and 10% other species (*Calluna vulgaris*, *Vaccinium vitis-idaea*, *Arctophylos uva-ursi*, *Empetrum nigrum*, *Vaccinium myrtillus*), whereas Kir-D hosts no bryophytes but 50% lichen species. *Vaccinium vitis-idaea* and various lichen species are also present in Sto-D, while Sto-M is additionally covered by *Vaccinium myrtillus* and *Calluna vulgaris*. All increment core samples from these microsites were cut using a microtome, TRW measured at 1/100 mm resolution using a LINTAB station (Rinn 2005), and samples crossdated considering standard dendrochronological techniques (Holmes 1983). Mean growth rates range from 0.83 mm/year in Kir-M to 0.97 mm/year in Kir-D, and from 1.00 mm/year in Sto-D to 1.15 mm/year in Sto-M, and mean tree ages range from 77 years in Kir-D to 83 years in Kir-M, and from 93 years in Sto-D to 119 years in Sto-M (for more details see D uthorn et al. 2013).

In each microsite, Kir-M, Kir-D, Sto-M and Sto-D, four trees (two cores per tree, pooled) were selected for stable isotope measurement considering the criteria of homogeneous growth, absence of missing rings, ring width > 0.01 mm, well-defined annual rings, and minimum age of 150 years. Hydrophilic extractives and lipophilic compounds were removed by purging the increment cores with distilled water and water-free ethanol for 8–24 h at 60 °C (Sidorova et al. 2008). Annual tree-rings covering the period 1901–2009 were truncated with a scalpel, and whole wood samples (Mischel et al. 2015; Riechelmann et al. 2014, 2016) of 300–3000 µg packed in tin capsules for stable carbon isotope measurement, and 250–300 µg samples in silver capsules for stable oxygen isotope measurement. The tin capsules were combusted in an elemental analyzer at 1150 °C, $^{13}\text{C}/^{12}\text{C}$ measured using an IsoPrime IRMS, and $\delta^{13}\text{C}$ expressed in parts per thousand (‰) with respect to an established reference material (Farquhar et al. 1982). For $\delta^{18}\text{O}$, the silver capsules were pyrolyzed at 1450 °C, $^{18}\text{O}/^{16}\text{O}$ quantified in an IRMS and expressed in ‰ relative to the standard isotopic composition of ocean water (Leavitt 2010). The analytical uncertainties of these data are $\pm 0.3\text{‰}$ for $\delta^{13}\text{C}$ and $\pm 0.5\text{‰}$ for $\delta^{18}\text{O}$, and the microsite chronologies denoted Kir ^{13}D , Kir ^{13}M , Kir ^{18}D , etc.

Numerous studies have applied $\delta^{13}\text{C}$ and $\delta^{18}\text{O}$ values in tree-ring material such as cellulose, lignin, whole wood or lignin methoxyl groups for climatic and environmental

studies (Barbour et al. 2001; Edwards and Fritz 1986; Gori et al. 2013; Loader et al. 2003; Mischel et al. 2015; Riechelmann et al. 2016). Acknowledging the findings of Wilson and Grinsted (1977) that tree-ring components have different isotopic ratios, most research has been carried out on single components, usually cellulose, and on single isotope proxies preferentially $\delta^{13}\text{C}$ and $\delta^{18}\text{O}$ (Boettger et al. 2007). However, the time-consuming cellulose extraction steps are still a disadvantage particularly in view of the need to develop long-term chronologies for climatic reconstruction. Alternatively, in recent years a number of studies have demonstrated the usefulness and effectiveness of $\delta^{13}\text{C}$, $\delta^2\text{H}$ and $\delta^{18}\text{O}$ of whole wood as a tree-ring climate proxy (Cullen and Grierson 2006; Gori et al. 2013; Loader et al. 2003; Mischel et al. 2015; Verheyden et al. 2005; Weigt et al. 2015). Gori et al. (2013) investigated *Picea abies* in alpine Italy and demonstrated that $\delta^{18}\text{O}$ and $\delta^2\text{H}$ from whole wood samples preserve the best temperature signals. Schleser et al. (2015) found a high correlation between $\delta^{13}\text{C}$ values from whole wood and extracted cellulose of tropical *Cariniana micrantha* over the past two and a half centuries, and Mischel et al. (2015) report on differences between whole wood and cellulose $\delta^{13}\text{C}$ and $\delta^{18}\text{O}$ timeseries of *Pinus sylvestris* supporting the choice to analyse whole wood instead of cellulose. For practical reasons and to substantially reduce costs, we measured $\delta^{13}\text{C}$ and $\delta^{18}\text{O}$ of the bulk tree-ring material of *Pinus sylvestris*.

Each $\delta^{13}\text{C}$ series was corrected for the Suess effect to remove a long-term declining trend since the mid-nineteenth century due to the combustion of fossil carbon and atmospheric enrichment of depleted CO_2 (Farquhar et al. 1989; Treydte et al. 2009). In addition, all isotopic data (including $\delta^{18}\text{O}$) were detrended using 30-year spline high-pass filters (Cook and Peters 1981) to remove level differences among single-tree isotope series and long-term trends that are potentially unrelated to climatic forcings. We use both versions of the data, the non-detrended (“raw”) and the spline-detrended (“spl”) stable isotope timeseries for calibration against instrumental climate data and report the highest agreements (Table 2). Gridded monthly mean temperatures, precipitation sums, cloud cover changes (Harris et al. 2014), and Palmer Drought Severity Index (PDSI; van der Schrier et al. 2006) reaching back to 1901 were used for calibration against tree-ring $\delta^{18}\text{O}$ and $\delta^{13}\text{C}$ using Pearson correlations. The gridded products were accessed through the KNMI climate explorer (Trouet and van Oldenborgh 2013; van Oldenborgh and Burgers 2005) at $0.5^\circ \times 0.5^\circ$ resolution and were employed to evaluate proxy climate signals over two overlapping intervals: 1901–2009 and 1951–2009. The latter period is used to evaluate the influence of potentially uncertain early instrumental data (Frank et al. 2007) as well as changes in proxy signal strength (Briffa et al. 1998b). Maps are produced highlighting correlations exceeding

Table 2 Best correlating seasonal instrumental data (JJA=June–August, Jan–Aug=January–August, Jul=July) and stable isotope data (Raw=non-detrended, Spl=spline-detrended) used in Figs. 6 and 7 for climate signal assessment

	Season		Detrending	
	Kir	Sto	Kir	Sto
Temperature				
$\delta^{13}\text{C}$	JJA	JJA	Spl	Spl
$\delta^{18}\text{O}$	Jul	Jan–Aug	Raw	Spl
Precipitation				
$\delta^{13}\text{C}$	JJA	JJA	Spl	Spl
$\delta^{18}\text{O}$	JJA	JJA	Spl	Spl
Cloud cover				
$\delta^{13}\text{C}$	JJA	JJA	Spl	Raw
$\delta^{18}\text{O}$	JJA	JJA	Spl	Spl
PDSI				
$\delta^{13}\text{C}$	JJA	JJA	Spl	Raw
$\delta^{18}\text{O}$	JJA	JJA	Raw	Raw

$p < 0.05$ to evaluate spatial patterns of climate signals. We also produced crossplots and linear regressions of selected isotope–climate associations and calculated 30-year running correlations to emphasize temporal changes in proxy climate signals.

Results and discussion

Average isotope ratios and covariance

On average, stable isotope ratios of tree-ring bulk wood increase by 0.8‰ ($\delta^{13}\text{C}$) and 2.4‰ ($\delta^{18}\text{O}$) from the Arctic tree line in northern Sweden towards Stockholm ~ 1000 km south of the ecotone, thereby verifying H1 for both proxies (Fig. 1). For oxygen, this offset is likely reflecting the temperature difference between northern and central Sweden (up to 10 °C), which controls the isotopic composition of atmospheric water supply (Kortelainen and Karhu 2004). Tree-ring $\delta^{18}\text{O}$ does, however, not change between the moist and dry microsities, disproving H2 on the influence of depleted groundwater for this proxy: immediate access to lake filtration water has no effect on average oxygen isotope signatures of pine tree-rings. Snowmelt as an important water source, particularly for trees at dry microsities and reaching far into the growing season (Treydte et al. 2014), likely affects the isotopic signature and differentiation between lakeshore and inland sites. This situation is different for $\delta^{13}\text{C}$, which is not only depleted in ^{13}C towards the arctic tree line (Hilasvuori et al. 2009; Stuiver and Braziunas 1987), but also from the dry to the moist microsities. The large-scale change is likely a representation of increased photosynthetic assimilation

in Sto, as reflected by wider tree-rings (average growth rate over the first 100 years of tree age in Sto = 1.10 mm, in Kir = 0.78 mm), regulating sub-stomatal CO_2 concentrations and forcing the leaf enzyme Rubisco to catalyze more of the heavy ^{13}C isotope (Saurer et al. 2004). At the local scale, the $\delta^{13}\text{C}$ offset is likely caused by prolonged stomatal resistance in the dry microsities during warm season drought periods of several days to weeks (Farquhar et al. 1989). The effect seems to be slightly stronger in the warmer Sto site, in which the offset between dry and wet microsities reaches 1.2‰, compared to only 0.7‰ in Kir.

The $\delta^{13}\text{C}$ offset between wet and dry microsities is also apparent in the annually resolved data covering the 20th and early twenty-first centuries (Fig. 2), though particularly in Kir-M (top panel) the differences between single trees are additionally noticeable. Besides these offsets, the annually resolved isotope data reveal highly coherent co-variability among trees and microsities, a key characteristic of these proxies building the foundation for high-resolution climate reconstruction (Frank et al. 2015; Kress et al. 2010; Treydte et al. 2006). Interseries correlations over 1901–2009 range from 0.48 to 0.69 for single trees and 0.74–0.85 for microsite chronologies (values shown in Fig. 2) substantiating the impact of common (climatic) forcings on inter-annual stable isotope variations. Interestingly, the mean interseries correlation is slightly higher among $\delta^{13}\text{C}$ and $\delta^{18}\text{O}$ series from wet microsities, though the difference is not substantial (0.08 across all sites) and not consistent ($\delta^{18}\text{O}$ in Sto).

To emphasize the high frequency (inter-annual to decadal) patterns in the isotope data, we detrended the $\delta^{13}\text{C}$ and $\delta^{18}\text{O}$ series using 30-year splines, and consider both the non-detrended and spl-detrended data for covariance and climate signal assessments. The detrending removes multi-decadal scale variability from the data (Fig. 3), and increases, on average, the covariance among microsities and across proxies (i.e. between $\delta^{13}\text{C}$ and $\delta^{18}\text{O}$) from 0.30 considering all non-detrended chronologies to 0.35 considering all detrended chronologies (Fig. 4). Besides the striking correlation between neighboring microsities, the matrix reveals significant correlations between carbon and oxygen isotopes within the study regions (Kir and Sto). Covariance between $\delta^{13}\text{C}$ and $\delta^{18}\text{O}$ is larger in Sto ($r = 0.39$) compared to Kir ($r = 0.28$), and particularly strong in Sto when considering only the spl-detrended chronologies ($r = 0.48$; the orange and yellow boxes in the two bottom rows of Fig. 4). The increased covariance in Sto reveals stomatal conductance, rather than photosynthesis, is the key driver of isotope fractionation in central Sweden. In comparison, the correlation between regions (Kir and Sto) for each proxy is relatively low ($r = 0.28$ for $\delta^{18}\text{O}$ and only 0.18 for $\delta^{13}\text{C}$) indicating that the data from central and northern Sweden are controlled by regionally differing climatic forcings. The overall higher correlations among the spl-detrended chronologies

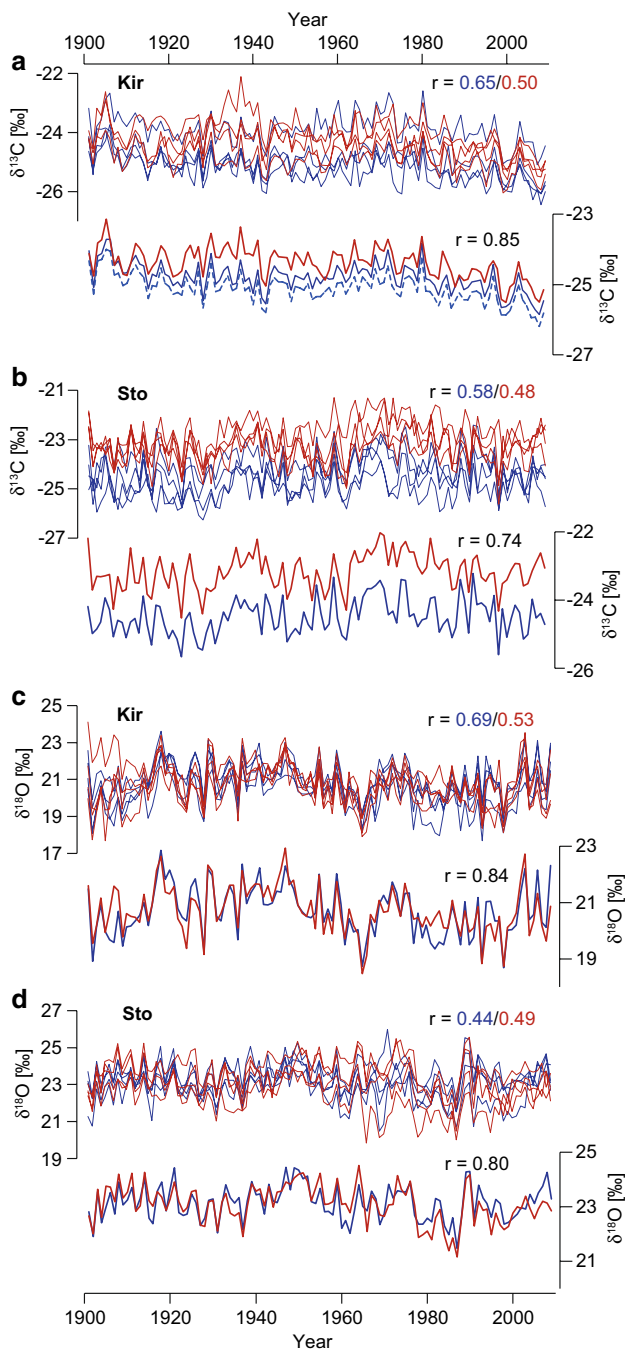


Fig. 2 Tree-ring $\delta^{13}\text{C}$ and $\delta^{18}\text{O}$ data 1901–2009. **a** $\delta^{13}\text{C}$ series of four trees in moist conditions (blue) and four trees in dry conditions (red) shown together with their mean chronologies (bottom panel). Dashed curve is the mean of only three trees excluding the data of one tree showing substantially less depleted values (top blue curve in top panel). Values are the inter-series correlations among trees at moist (blue) and dry (red) sites, as well as between the microsite chronologies (black). **b–d** Same as in **a**, but for $\delta^{13}\text{C}$ from Sto (**b**), $\delta^{18}\text{O}$ from Kir (**c**), and $\delta^{18}\text{O}$ from Sto (**d**)

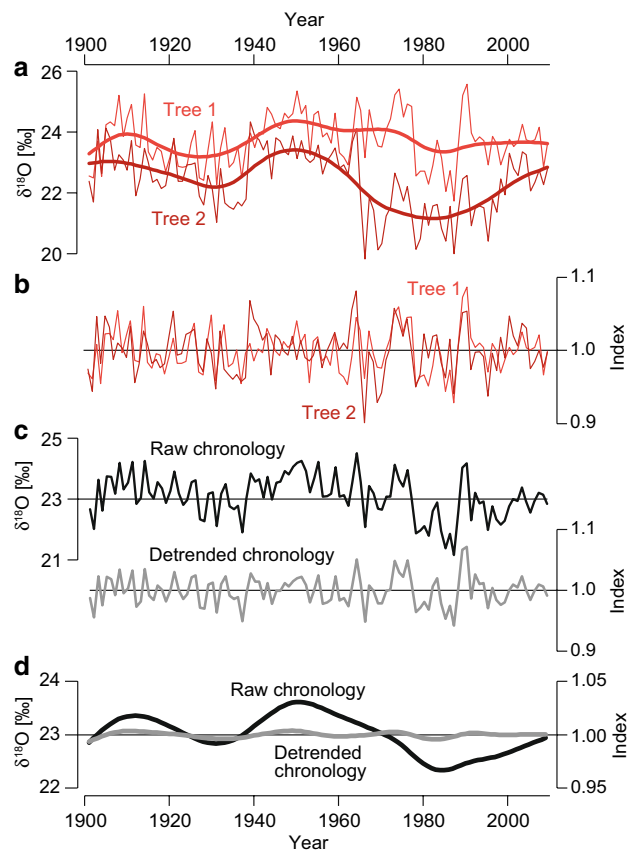


Fig. 3 Effects of detrending tree-ring stable isotope data. **a** $\delta^{18}\text{O}$ series of two trees from Sto-D (thin curves) shown together with their 30-spline low pass filters (thick curves). **b** Detrended $\delta^{18}\text{O}$ series of the two trees derived from calculating ratios between the original measurements and spline filters shown in **a**. **c** Mean $\delta^{18}\text{O}$ raw (black curve) and detrended (grey curve) chronologies of four trees at Sto-D. **d** 30-year low pass filters of the detrended and non-detrended chronologies

Raw / Spl	Kiruna				Stockholm			
	^{13}M	^{13}D	^{18}M	^{18}D	^{13}M	^{13}D	^{18}M	^{18}D
Kiruna ^{13}M		0.85	0.13	0.22	0.17	0.15	0.03	0.18
Kiruna ^{13}D	0.86		0.28	0.30	0.15	0.19	0.01	0.13
Kiruna ^{18}M	0.37	0.39		0.84	0.21	0.18	0.35	0.29
Kiruna ^{18}D	0.31	0.25	0.85		0.22	0.18	0.34	0.32
Stockholm ^{13}M	0.21	0.20	0.41	0.39		0.74	0.39	0.24
Stockholm ^{13}D	0.18	0.23	0.31	0.27	0.71		0.38	0.20
Stockholm ^{18}M	0.13	0.05	0.24	0.25	0.53	0.53		0.80
Stockholm ^{18}D	0.10	0.02	0.20	0.25	0.41	0.43	0.83	

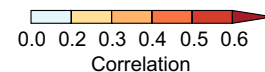


Fig. 4 Correlation coefficients between $\delta^{13}\text{C}$ and $\delta^{18}\text{O}$ microsite chronologies from Kiruna and Stockholm using the non-detrended (Raw) and spline-detrended (Spl) data from 1901 to 2009. Considering the varying lag-1 autocorrelations of these data, $p < 0.05$ is reached at $r \approx 0.22$ for the non-detrended and $r \approx 0.19$ for the detrended data

demonstrate that cross-proxy and cross-microsite variance is most coherent at inter-annual timescale, and supports findings indicating strong climate signals in the high frequency domain across Europe (Treydte et al. 2007).

Climate signals

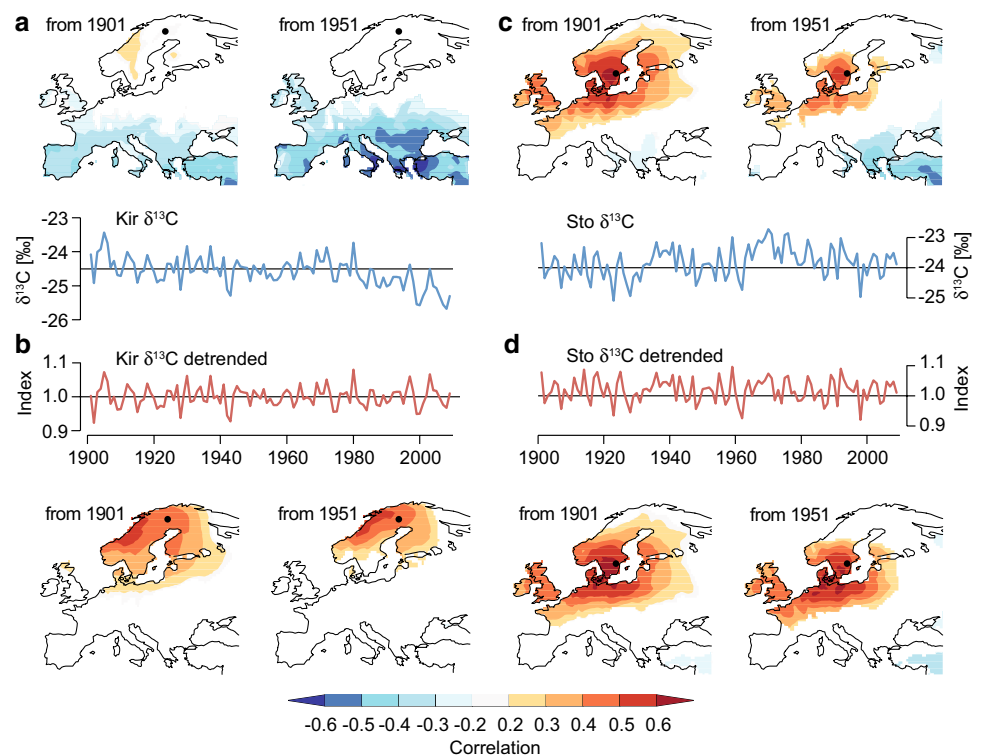
The removal of trends from proxy timeseries is also known to potentially affect the climate signals estimated via the calibration against instrumental climate data (Fritts 1976). The modification caused by detrending can be small, such as expressed in a spatially expanded temperature correlation field recorded for Sto $\delta^{13}\text{C}$ over the late 1951–2009 calibration period (Fig. 5c, d), but might also radically change the putative signal, from insignificant in the vicinity of the proxy location to a noticeable temperature response after detrending (Fig. 5a, b). In this latter example of $\delta^{13}\text{C}$ from Kir, the recent negative trend in the raw data accidentally resulted in the detection of inverse temperature correlations in southern Europe, reminding of the danger of picking up spurious patterns when using auto-correlated data (Esper et al. 2005; von Storch et al. 2004).

Bearing these modifications related to timeseries detrending in mind, we calibrated all $\delta^{13}\text{C}$ and $\delta^{18}\text{O}$ microsite chronologies against gridded temperature, precipitation, cloud cover, and PDSI data over the 1901–2009 and 1951–2009 periods using Pearson correlations and illustrate the most significant fields (Figs. 6, 7). In most cases,

highest correlations are achieved when averaging the instrumental data over the summer months (JJA), except for the temperature-versus- $\delta^{18}\text{O}$ pair, which is showing strongest responses during July in Kir and January–August in Sto (Table 2). Similarly, the spl-detrended stable isotopes more often correlate superior with instrumental fields, i.e. in only 5 of 16 cases the non-detrended data return stronger signals. While not highly significant, this finding indicates that the coherence with climate parameters can increase when removing inter-decadal scale variance from stable isotope records.

Even though the strength and spatial extent of correlation differ among the climate parameters tested here, significant fields are present for almost all proxy-climate pairs (Figs. 6, 7). This correlation with multiple instrumental datasets is seemingly affected by the covariance among climate parameters, making it difficult to differentiate between truly controlling and co-varying forcings (Biondi and Waikul 2004; Fritts et al. 1971). Comparisons between PDSI and Kir ^{13}M and Kir ^{13}D are non-significant when calculated over the long 1901–2009 calibration period, but the significant association evident for the 1951–2009 period (bottom-left in Fig. 6) implies potential deficiencies in the early instrumental network over northern Sweden. In other cases, the correlation fields do not match the tree sites, but are situated northeast (Kir $\delta^{13}\text{C}$ and cloud cover) and east (Sto $\delta^{13}\text{C}$ and cloud cover) of the sampling locations. These spatially disconnected patterns might reflect

Fig. 5 Effects of stable isotope detrending on the calibration against instrumental climate data. **a** Spatial patterns of the correlation of the non-detrended Kir $\delta^{13}\text{C}$ site chronology (blue curve) against gridded instrumental JJA temperatures from 1901 to 2009 (top left) and 1951–2009 (top right). **b–d** Same as in **a**, but for the detrended Kir $\delta^{13}\text{C}$ (**c**), non-detrended Sto $\delta^{13}\text{C}$ (**c**), and detrended $\delta^{13}\text{C}$ chronologies (**d**). Significant correlation $p < 0.10$ displayed



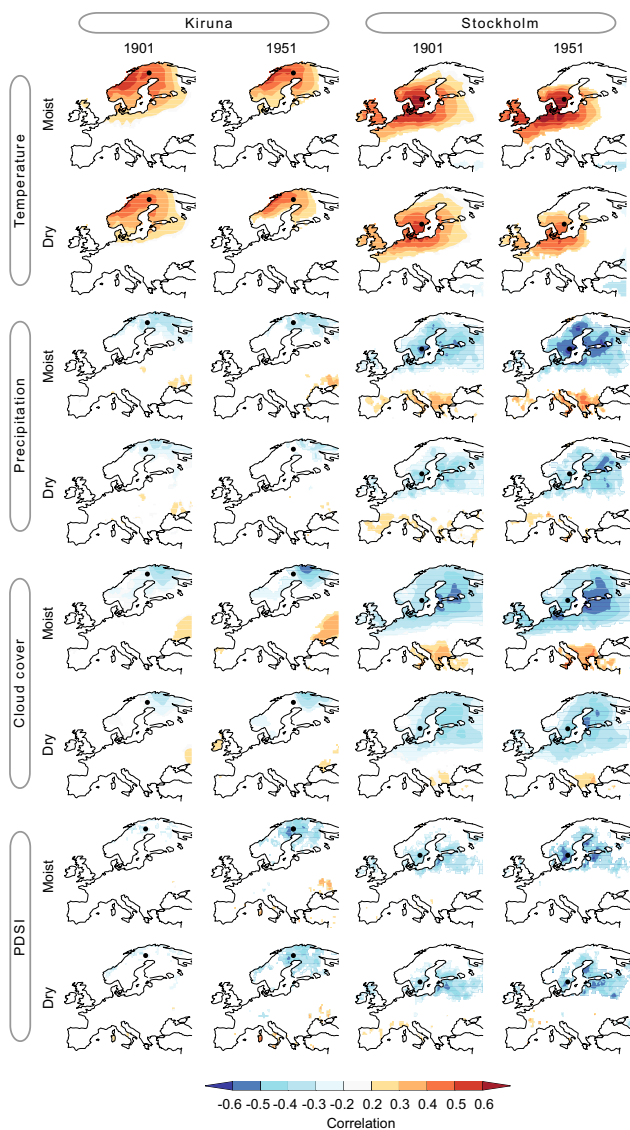


Fig. 6 Climate signals in $\delta^{13}\text{C}$ data from locally dry and locally moist sites in Kir and Sto. Correlation fields for the periods 1901–2009 and 1951–2009 (columns) for temperature, precipitation, cloud cover, and PDSI (rows) are shown. For each combination, only the best-correlating season and data (detrended or non-detrended) are illustrated. Significant correlation $p < 0.10$ displayed. See Table 2 for details

deficiencies in the cloud data network, since remote influences of cloud-controlled irradiance on tree-ring isotope formation are unlikely. An extreme case is the temperature pattern associated with Kir $\delta^{18}\text{O}$ (top left in Fig. 7), where the correlation field is centered ~1000 km south of the tree site. The argument that instrumental data are defective might be somewhat circumstantial here (since temperature readings are typically more robust compared to hydroclimatic and insolation parameters; Auer et al. 2007; Böhm et al. 2001), and the remote correlation field might rather reflect a true signal related to prevailing air

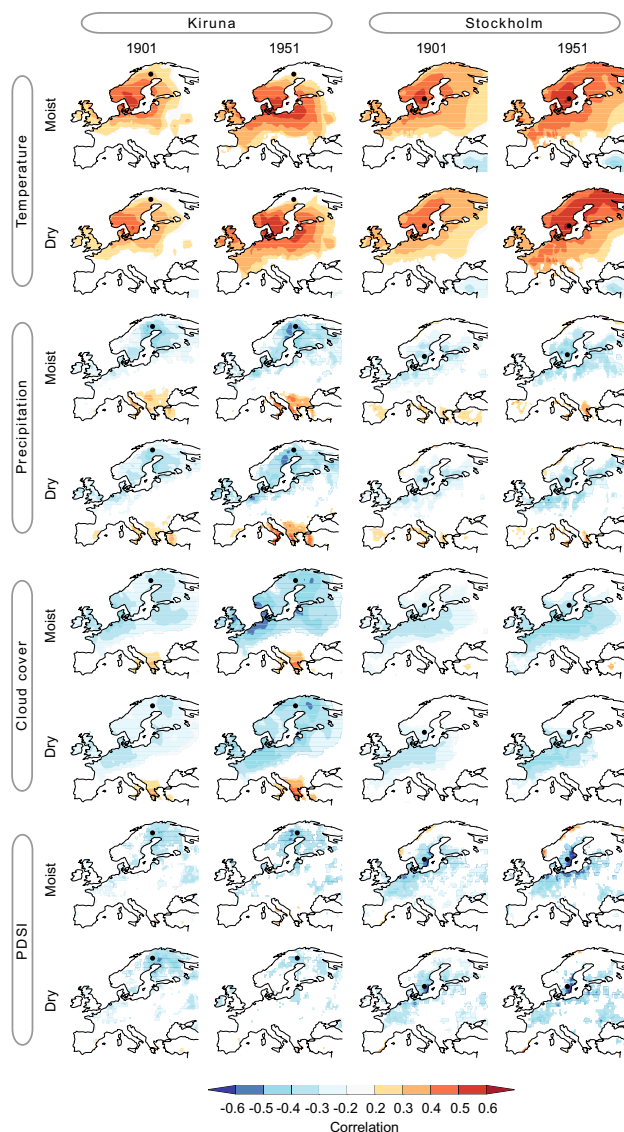


Fig. 7 Climate signals in $\delta^{18}\text{O}$ data from locally moist and locally wet sites in Kir and Sto. Correlation fields for the periods 1901–2009 and 1951–2009 (columns) for temperature, precipitation, cloud cover, and PDSI (rows) are shown. For each combination, only the best-correlating season and data (detrended or non-detrended) are illustrated. Significant correlation $p < 0.10$ displayed. See Table 2 for details

mass trajectories and their impact on precipitation $\delta^{18}\text{O}$ signatures (see next section).

After considering all proxy-instrumental data combinations, it is evident that the highest correlations are recorded for warm season temperatures, except for Sto $\delta^{18}\text{O}$ correlating best with PDSI (Fig. 8). Importantly, in almost all cases, the stable isotope records from moist microsites correlate better with climate parameters compared to the data from their neighboring dry sites. The few exceptions include temperature signals in Kir $\delta^{18}\text{D}$ and Sto $\delta^{18}\text{D}$ from 1951 to 2009 and the (overall weak) PDSI

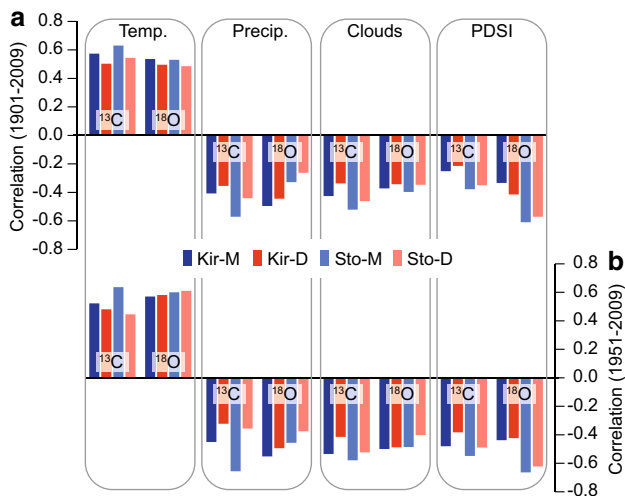


Fig. 8 Stable isotope climate signals. **a** Pearson correlation coefficients of $\delta^{13}\text{C}$ and $\delta^{18}\text{O}$ microsite chronologies (moist sites in blue, dry sites in red) from Kiruna (dark colors) and Stockholm (light colors) against instrumental temperature, precipitation, cloud cover, and PDSI data (seasons specified in Table 2) considering the best-correlating grid-points shown in Figs. 6 and 7 from 1901 to 2009. Considering varying lag-1 autocorrelations, $p < 0.05$ is reached at $r \approx 0.19$. **b** Same as in **a**, but over the 1951–2009 period. $p < 0.05$ is reached at $r \approx 0.27$

signal in Kir¹³D, which are slightly stronger compared to their moist counterparts. The correlation difference between moist and dry microsites is mostly insignificant and reaches, on average, 0.07 (0.12) for $\delta^{13}\text{C}$ and 0.05 (0.05) for $\delta^{18}\text{O}$ over the 1901–2009 (1951–2009) calibration period. This small, but fairly systematic, modification between moist and dry microsites likely originates from differentiating effects of groundwater access on the climatic signal strength of carbon and oxygen isotopes as formulated in hypothesis H3.

These effects appear to be stronger in Sto compared to Kir (particularly $\delta^{18}\text{O}$ from 1951 to 2009) as well as in $\delta^{13}\text{C}$ compared to $\delta^{18}\text{O}$. Access to lake infiltration water allows for stronger stomatal conductance even during warm and dry periods, a process that not only reinforces atmospheric control of oxygen and carbon fractionation (Darling and Talbot 2003; Leavitt and Long 1989; Saurer et al. 1995), but is also more effective at the warmer Sto site in central Sweden compared to Kir at the Arctic tree line. As a consequence, isotope-based climate reconstructions of warm season temperature (but also precipitation, cloud cover, and PDSI) would explain more variance of the targeted climate variable, if trees from locally moist microsites were considered. When developing composite chronologies integrating isotopic data from living and sub-fossil trees (e.g., Hangartner et al. 2012), it seems therefore important to avoid changes in microsite habitats. Mixing microsites in millennium-scale chronologies could otherwise result in temporal changes in

reconstruction skill that seem difficult to be statistically estimated.

Correlation with TRW data

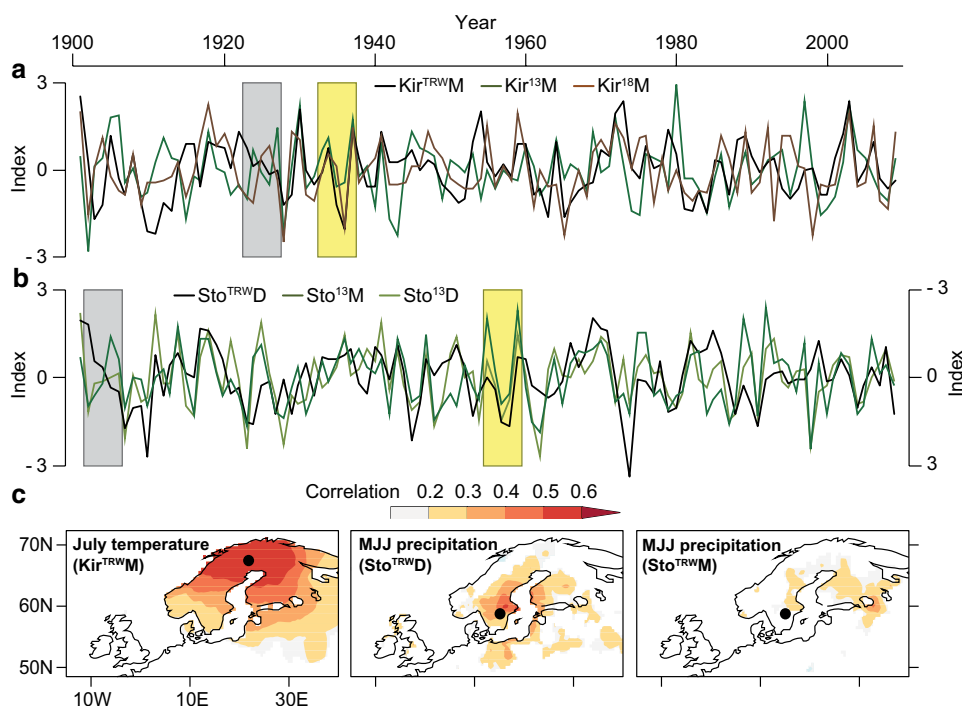
While we acknowledge the difficulty of differentiating between leading and co-varying climate variables controlling stable isotope composition (Frank et al. 2015), comparison with TRW data from the same trees might offer some support to our interpretation of $\delta^{13}\text{C}$ and $\delta^{18}\text{O}$ records. Figure 9 shows the correlation of Kir¹³M and Kir¹⁸M with Kir^{TRW}M, and the anti-correlation between TRW from the dry microsite (Sto^{TRW}D) with Sto¹³D and Sto¹³M from 1901 to 2009. The coherent decadal scale variance and significant correlation between stable isotopes and TRW data in the Arctic Kir-M environment (Kir¹⁸M/Kir^{TRW}M = 0.44, Kir¹³M/Kir^{TRW}M = 0.33; Fig. 9a) is in line with the calibration against warm season temperatures (Büntgen et al. 2011; Esper et al. 2013, 2014; Linderholm et al. 2015). Interestingly, cross-proxy correlation in this cold environment is stronger in the moist microsite as both the lakeshore stable isotope (Fig. 8) and TRW data (Düthorn et al. 2016) contain stronger temperature signals, compared to their inland counterparts.

This situation is different in the overall warmer Sto site, where temperature-controlled $\delta^{13}\text{C}$ (from moist and dry microsites) correlates negatively with precipitation-controlled TRW from the dry microsite (Fig. 9b, $r = -0.38$ for Sto¹³M, and $r = -0.45$ for Sto¹³D). TRW data from the moist microsite in Sto contains no clear precipitation signal (compare middle and right panels in Fig. 9c), likely because groundwater access degrades the influence of rainfall events on pine cambial activity (Düthorn et al. 2015, 2016). As a consequence, Sto^{TRW}M and Sto^{TRW}D correlate at only $r = 0.42$, whereas Kir^{TRW}M and Kir^{TRW}D, located north of the Arctic Circle, correlate at $r = 0.84$. Finally, it seems noticeable that lag-1 autocorrelations differ systematically between the proxies displayed in Fig. 9 ranging from < 0.05 for all isotope chronologies to 0.30 in Kir^{TRW}M and 0.43 in Sto^{TRW}D (all after spl-detrending). High serial correlation is characteristic for TRW chronologies (Matalas 1962; Meko 1981) and limits the ability to properly assess distinct temperature extremes (Esper et al. 2015b). This situation is seemingly different in $\delta^{13}\text{C}$ and $\delta^{18}\text{O}$, which could offer a pathway to improve the reconstruction of cooling events following large volcanic eruptions and other abrupt climate changes (Briffa et al. 1998a; Esper et al. 2013; Schneider et al. 2015).

Temperature and cloud cover signals

Two obvious applications arising from our results would be, first, the reconstruction of large-scale temperature patterns

Fig. 9 Stable isotope versus tree-ring width comparison. **a** Kir¹³M and Kir¹⁸M chronologies shown together with the TRW chronology from the same four trees in locally moist conditions (Kir^{TRW}M). All data detrended using 30-year spline high-pass filters. Grey and yellow boxes mark periods of reduced (1923–1927) and increased (1933–1937) covariance, respectively. **b** Same as in **a**, but for the Sto¹³M, Sto¹³D, and Sto^{TRW}D chronologies (TRW axis on the right reversed). Grey and yellow boxes highlight 1902–1906 and 1955–1959. **c** Maps showing the correlation between Kir^{TRW}M and July temperature (left), Sto^{TRW}D and MJJ precipitation, and Sto^{TRW}M and MJJ precipitation over the 1901–2009 period

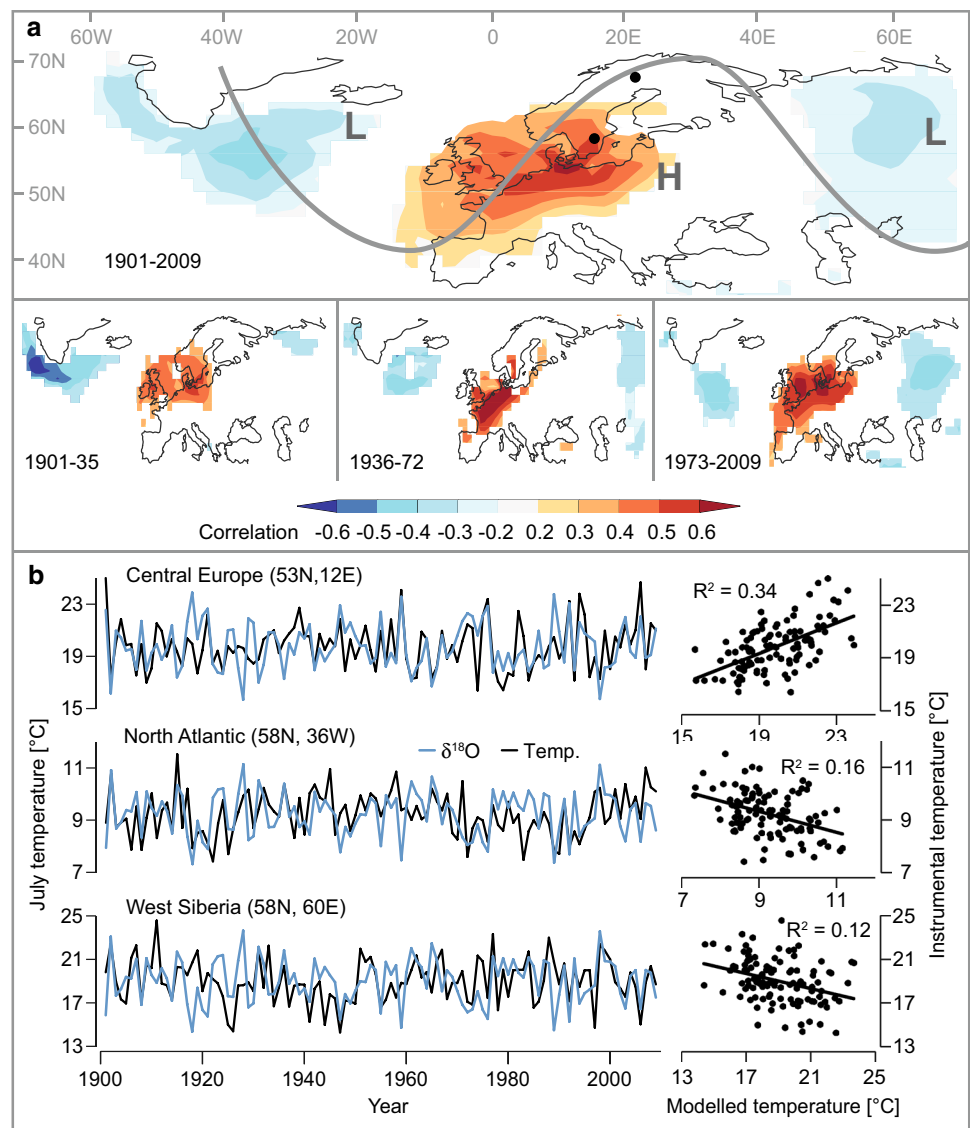


from $\delta^{18}\text{O}$, and second, estimates of past changes in insolation and cloud cover. The notable temperature correlation centered over northern Germany, reflected in both Kir¹³M and Sto¹³M, is coupled with significant, but inverse correlation fields in the North Atlantic and west Siberia (Fig. 10). These associations are physically meaningful as surface temperatures in these regions (North Atlantic, central Europe, west Siberia) are teleconnected via the westerlies steered by the polar jet stream (Ahrens 2012; Flohn 1950). The prevailing vectors of this planetary wind circulation (shown in grey in Fig. 10) are closely linked with the position and strength of the semi-permanent Icelandic low and Russian high. The combination of $\delta^{18}\text{O}$ data from Kir-M and Sto-M thereby offers the opportunity to reconstruct changes in the strength and position of these synoptic systems relevant to weather and climate of a large fraction of the Northern Hemisphere (Wanner et al. 2001). We assume that a stronger zonal component of the planetary circulation would be reflected by a weakening of the anti-correlation among the Atlantic, European, Siberian sectors, whereas a stronger meridional component would strengthen these teleconnections. Such temporal changes could be studied using split calibration windows as shown in the bottom panel of Fig. 10a, but clearly more proxy data are needed to explore the potential of reconstructing such atmospheric dynamics with statistical skill (Luterbacher et al. 2002; Trouet et al. 2009, 2016).

The insolation signal inherent to stable carbon isotopes from northern Scandinavia has been thoroughly explored by calibrating against local sunshine data recorded in Abisko in northern Sweden (Loader et al. 2013). Loader

et al. (2013) show that in northern boreal forests stomatal control of CO_2 diffusion into the leaves is less affected by moisture stress, but photosynthetically active radiation is the primary limiting factor controlling carbon isotope fractionation. The extremely high correlation between sunshine hour and cloud cover (typically > 0.90 ; Barbaro et al. 1981; Ododo et al. 1996; Reddy 1974) is the main justification for merging these different observations of solar insolation into gridded products covering global land areas (New et al. 2002). Our $\delta^{13}\text{C}$ data from Kir-M and Sto-M revealed that the centers of correlation with cloud cover/sunshine hour data are displaced and shifted towards northeast (Kir¹³M) and east (Sto¹³M). Interestingly, the sunshine hour data from the Abisko climate station also correlate with gridded cloud data centered in northwest Finland (Fig. 11a). These remote correlation fields seen in both proxy and instrumental data likely indicate paucities in the gridded cloud cover network (New et al. 2002), limiting efforts to reconstruct long-term insolation variability based on tree-ring stable isotopes. This conclusion is supported by temporal correlation changes signifying skill deterioration in the gridded cloud cover data before 1960 (Fig. 11b). In addition, since both Kir¹³M and $\delta^{13}\text{C}$ from Loader et al. (2013) reveal a correlation drop against Abisko sunshine hours centered in the 1950s, the validation of proxy insolation signals based on the calibration against observational data remains challenging. The main reason for this failure is likely the low and temporally varying quality of observational cloud cover and sunshine hour data. This being said, the previously detailed temperature and PDSI signals (Figs. 6, 7, 8) might merely appear

Fig. 10 Large-scale $\delta^{18}\text{O}$ correlation patterns. **a** Correlation fields of the mean oxygen-moist chronology ($\text{Kir}^{18}\text{M} + \text{Sto}^{18}\text{M}$) against gridded instrumental JJA land and sea surface temperatures (SST) from 1901 to 2009 (top panel). Bottom panel shows the fields for 1901–1935, 1936–1972, and 1973–2009. Significant correlations $p < 0.10$ are displayed. **b** Mean $\delta^{18}\text{O}$ -moist chronology (blue curve) scaled to JJA temperatures in Europe (black curve; 53°N , 12°E) together with a scatter plot and linear regression of the data (top panel). Middle and bottom panels show the $\delta^{18}\text{O}$ -moist data scaled to SSTs from the North Atlantic (58°N , 36°W) and land temperatures from west Siberia (58°N , 60°E)



superior because thermometer readings contain fewer biases compared to cloud cover, sunshine hour, and precipitation data (Auer et al. 2007).

Conclusions

The analysis of pine tree-ring $\delta^{13}\text{C}$ and $\delta^{18}\text{O}$ data from moist and dry microsites in Scandinavia revealed small but systematic differences in climate signal strength. Stable isotopes from moist microsites correlate better (on average by 0.09 for $\delta^{13}\text{C}$ and 0.05 for $\delta^{18}\text{O}$) against gridded climate data compared to their dry counterparts, a finding that is largely robust for temperature, precipitation, cloud cover, and PDSI. Access to lake filtration water also depleted $\delta^{13}\text{C}$ by $\sim 1\%$, but did not affect $\delta^{18}\text{O}$. In contrast, both isotope values increased from the warmer sampling site near Stockholm

to the colder site near the Arctic tree line located ~ 1000 km north of the Swedish capital ($\delta^{13}\text{C}$ by 0.8% and $\delta^{18}\text{O}$ by 2.4%). These large-scale gradients are caused by temperature controlled changes in the isotopic composition of meteoric water ($\delta^{18}\text{O}$) and assimilation controlled enzymatic fractionation processes ($\delta^{13}\text{C}$).

We found significant correlations between all stable isotope microsite chronologies and all tested climatic parameters. In most microsites, $\delta^{13}\text{C}$ and $\delta^{18}\text{O}$ agreed best with warm season temperature. An exception is $\delta^{18}\text{O}$ from the dry microsite in central Sweden, where needle aperture in trees with limited soil water access more closely regulates CO_2 , a mechanism that is best reflected in PDSI data (van der Schrier et al. 2006). The overall strong climatic forcing synchronized stable isotope variance among single trees and microsites. Covariance even increased after high-pass filtering the proxy data, reinforcing signal strength of tree-ring

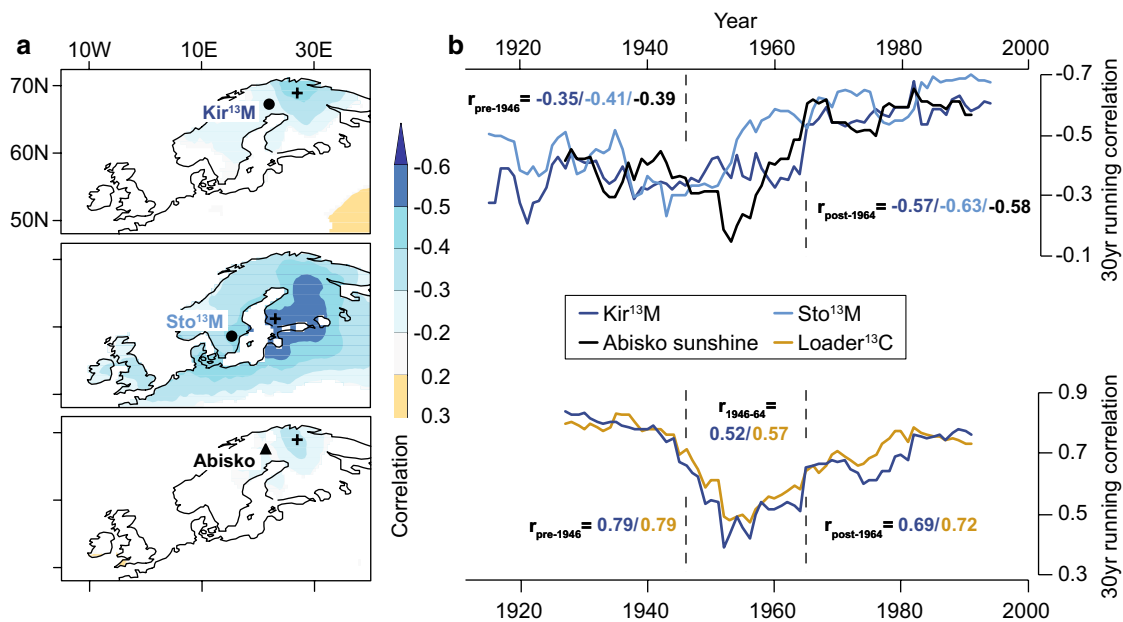


Fig. 11 Stable isotope cloud cover and sunshine hour signals. **a** Spatial pattern of the correlation between Kir¹³M and gridded JJA cloud cover data from 1913 to 2006 (top panel). Middle panel shows the correlation pattern for Sto¹³M, and bottom panel shows the pattern for JJA sunshine hour data recorded at the Abisko climate station from 1913 to 2006. The crosses indicate the grid point used for calculating running correlations shown in **b**. **b** 30-year running correlations between Kir¹³M and JJA cloud cover at 69°N and 28°E (see cross in

a, top panel) in dark blue, Sto¹³M and JJA cloud cover at 61°N and 22°E (cross in **a**, middle panel) in light blue, and Abisko JJA sunshine hours with JJA cloud cover at 69°N and 28°E (cross in **a**, bottom panel) in black. Bottom panel shows the 30-year running correlations between Kir¹³M and the nearby JJA sunshine hour data recorded in Abisko (1913–2006) in dark blue, and between the Loader et al. (2013) δ¹³C data from Torneträsk and Abisko JJA sunshine hours

δ¹³C and δ¹⁸O chronologies for reconstructing abrupt climatic changes. Covariance is also substantial between δ¹³C and δ¹⁸O chronologies within each region (central and northern Sweden) underpinning that similar climate forcings influence these proxies (Treydte et al. 2007; Saurer et al. 2008).

A conclusive differentiation between forcing and co-varying climate parameters seemed challenging based on only the calibration against instrumental climate data. Covariance of δ¹³C and δ¹⁸O with (temperature controlled) TRW data in northern Sweden, and δ¹³C with (drought controlled) TRW data in central Sweden, however, supported the climatic interpretation of tree-ring stable isotopes as temperature and PDSI proxies, particularly in the high frequency domain. On the other hand, a physiologically perhaps more meaningful cloud cover reconstruction appeared to be constrained by the mediocrity of twentieth century observational data precluding signal strength assessments particularly in the low frequency domain.

Author contribution statement The study was conducted in collaboration between all authors: JE and SH designed the study and carried out most calculations. KT, UB, CHM, SSG and DFCR supported the interpretation, and BS and FK contributed to the laboratory work. The discussion and

conclusions were a joint work among all authors. The manuscript was written by JE and revised by all other authors.

Acknowledgements We thank Florian Benninghoff, Willy Dindorf, Elisabeth Dühorn, Susanne Koch, Markus Kochbeck, Oliver Konter, Michael Maus, Maria Mischel and Jutta Sonnberg for field and laboratory support.

Compliance with ethical standards

Conflict of interest All authors declare no conflict of interest.

References

- Ahrens CD (2012) Meteorology today: an introduction to weather, climate, and the environment. Brooks/Cole, Belmont
- Auer I et al (2007) HISTALP—historical instrumental climatological surface time series of the greater Alpine region 1760–2003. *Int J Climatol* 27:17–46
- Barbaro S, Cannata G, Coppolino S, Leone C, Sinagra E (1981) Correlation between relative sunshine and state of the sky. *Sol Energy* 26:537–550
- Barbour MM (2007) Stable oxygen isotope composition of plant tissue: a review. *Funct Plant Biol* 34:83–94

- Barbour MM, Andrews TJ, Farquhar GD (2001) Correlations between oxygen isotope ratios of wood constituents of *Quercus* and *Pinus* samples from around the world. *Funct Plant Biol* 28:335–348
- Bégin C, Gingras M, Savard MM, Marion J, Nicault A, Bégin Y (2015) Assessing tree-ring carbon and oxygen stable isotopes for climate reconstruction in the Canadian northeastern boreal forest. *Palaeogeogr Palaeoclimatol Palaeoecol* 423:91–101
- Biondi F, Waikul K (2004) Dendroclim2002: a C++ program for statistical calibration of climate signals in tree-ring chronologies. *Computers Geosci* 30:303–311
- Boettger T et al (2007) Wood cellulose preparation methods and mass spectrometric analyses of $\delta^{13}\text{C}$, $\delta^{18}\text{O}$ and non-exchangeable $\delta^2\text{H}$ values in cellulose, sugar, and starch: an inter-laboratory comparison. *Anal Chem* 79:4603–4612
- Böhm R, Auer I, Brunetti M, Maugeri M, Nanni T, Schöner W (2001) Regional temperature variability in the European Alps 1760–1998 from homogenized instrumental time series. *Int J Climatol* 21:1779–1801
- Briffa KR, Jones PD, Schweingruber FH, Osborn TJ (1998a) Influence of volcanic eruptions on Northern Hemisphere summer temperature over the past 600 years. *Nature* 393:450–455
- Briffa KR, Schweingruber FH, Jones PD, Osborn TJ, Shiyatov SG, Vaganov EA (1998b) Reduced sensitivity of recent tree-growth to temperature at high northern latitudes. *Nature* 391:678–682
- Büntgen U et al (2011) Causes and consequences of past and projected Scandinavian summer temperatures, 500–2100 AD. *Plos One*. <https://doi.org/10.1371/journal.pone.0025133>
- Cernusak LA, English NB (2015) Beyond tree-ring widths: stable isotopes sharpen the focus on climate responses of temperate forest trees. *Tree Phys*. <https://doi.org/10.1093/treephys/tpu115>
- Cook ER, Peters K (1981) The smoothing spline: a new approach to standardizing forest interior tree-ring width series for dendroclimatic studies. *Tree-Ring Bull* 41:45–54
- Cook ER et al (2015) Old world megadroughts and pluvials during the Common Era. *Sci Adv*. <https://doi.org/10.1126/sciadv.1500561>
- Cullen LE, Grierson PF (2006) Is cellulose extraction necessary for developing stable carbon and oxygen isotopes chronologies from *Callitris glaucophylla*? *Palaeogeogr Palaeoclimatol Palaeoecol* 236:206–216
- Dansgaard W (1964) Stable isotopes in precipitation. *Tellus* 16:436–468
- Darling WG, Talbot JC (2003) The O & H stable isotopic composition of fresh waters in the British Isles. 1. Rainfall. *Hydrol Earth Syst Sci* 7:163–181
- Düthorn E, Holzkämper S, Timonen M, Esper J (2013) Influence of micro-site conditions on tree-ring climate signals and trends in Central and Northern Sweden. *Trees* 27:1395–1404
- Düthorn E, Schneider L, Konter O, Schön P, Timonen M, Esper J (2015) On the hidden significance of differing micro-sites in dendroclimatology. *Silva Fenn*. <https://doi.org/10.14214/sf.1220>
- Düthorn E, Schneider L, Günther B, Gläser S, Esper J (2016) Ecological and climatological signals in tree-ring width and density chronologies along a latitudinal boreal transect. *Scand J For Res* 31:750–757
- Edwards TWD, Fritz P (1986) Assessing meteoric water composition and relative humidity from ^{18}O and ^2H in wood cellulose: paleoclimatic implications for southern Ontario, Canada. *Appl Geochem* 1:715–723
- Ehleringer JR, Dawson TE (1992) Water-uptake by plants—perspectives from stable isotope composition. *Plant Cell Environ* 15:1073–1082
- Esper J, Frank DC, Wilson RJS, Briffa KR (2005) Effect of scaling and regression on reconstructed temperature amplitude for the past millennium. *Geophys Res Lett*. <https://doi.org/10.1029/2004GL021236>
- Esper J, Frank DC, Büntgen U, Verstege A, Luterbacher J, Xoplaki E (2007) Long-term drought severity variations in Morocco. *Geophys Res Lett*. <https://doi.org/10.1029/2007GL030844>
- Esper J, Frank DC, Battipaglia G, Büntgen U, Holert C, Treydte K, Siegwolf R, Saurer M (2010) Low-frequency noise in $\delta^{13}\text{C}$ and $\delta^{18}\text{O}$ tree ring data: a case study of *Pinus uncinata* in the Spanish Pyrenees. *Glob Biogeochem Cycl*. <https://doi.org/10.1029/2010GB0037772>
- Esper J, Schneider L, Krusic PJ, Luterbacher J, Büntgen U, Timonen M, Sirocko F, Zorita E (2013) European summer temperature response to annually dated volcanic eruptions over the past nine centuries. *Bull Volcanol*. <https://doi.org/10.1007/s00445-013-0736-z>
- Esper J, Düthorn E, Krusic P, Timonen M, Büntgen U (2014) Northern European summer temperature variations over the Common Era from integrated tree-ring density records. *J Quat Sci* 29:487–494
- Esper J, Konter O, Krusic P, Saurer M, Holzkämper S, Büntgen U (2015a) Long-term summer temperature variations in the Pyrenees from detrended stable carbon isotopes. *Geochronom* 42:53–59
- Esper J, Schneider L, Smerdon J, Schöne B, Büntgen U (2015b) Signals and memory in tree-ring width and density data. *Dendrochronologia* 35:62–70
- Esper J et al (2016) Review of tree-ring based temperature reconstructions of the past millennium. *Quat Sci Rev* 145:134–151
- Farquhar G, Roderick M (2007) Worldwide changes in evaporative demand. *Water Environ Scripta Varia* 108:81–103
- Farquhar GD, O’Leary MH, Berry JA (1982) On the relationship between carbon isotope discrimination and the intercellular carbon dioxide concentration in leaves. *Funct Plant Biol* 9:121–137
- Farquhar GD, Ehleringer R, Hubic KT (1989) Carbon isotope discrimination and photosynthesis. *Annu Rev Plant Physiol Plant Mol Biol* 40:503–537
- Flohn H (1950) Neue Anschauungen über die allgemeine Zirkulation der Atmosphäre und ihre klimatische Bedeutung. *Erdkunde* 141–162
- Frank D, Büntgen U, Böhm R, Maugeri M, Esper J (2007) Warmer early instrumental measurements versus colder reconstructed temperatures: shooting at a moving target. *Quat Sci Rev* 26:3298–3310
- Frank DC et al (2015) Water use efficiency and transpiration across European forests during the Anthropocene. *Nature Clim Change* 5:579–583
- Friedrichs DA, Büntgen U, Frank DC, Esper J, Neuwirth B, Löffler J (2008) Complex climate controls on 20th century oak growth in Central-West Germany. *Tree Phys* 29:39–51
- Fritts HC (1976) *Tree rings and climate*. Academic, New York
- Fritts HC, Blasing TJ, Hayden BP, Kutzbach JE (1971) Multivariate techniques for specifying tree-growth and climate relationships and for reconstructing anomalies in paleoclimate. *J Appl Meteorol* 10:845–864
- Gagen M, McCarroll D, Edouard JL (2004) Latewood width, maximum density, and stable carbon isotope ratios of pine as climate indicators in a dry subalpine environment, French Alps. *Arct Antarct Alp Res* 36:166–171
- Gagen M, Zorita E, McCarroll D, Young GH, Grudd H, Jalkanen R, Loader NJ, Robertson I, Kirchhefer A (2011) Cloud response to summer temperatures in Fennoscandia over the last thousand years. *Geophys Res Lett*. <https://doi.org/10.1029/2010GL046216>
- Gessler A, Ferrio JP, Hommel R, Treydte K, Werner RA, Monson RK (2014) Stable isotopes in tree rings: towards a mechanistic understanding of isotope fractionation and mixing processes from the leaves to the wood. *Tree Phys* 34:796–818
- Gori YURI., Wehrens R, Greule M, Keppler F, Ziller L, La Porta N, Camin F (2013) Carbon, hydrogen and oxygen stable isotope ratios of whole wood, cellulose and lignin methoxyl groups

- of *Picea abies* as climate proxies. *Rap Comm Mass Spectr* 27:265–275
- Hangartner S, Kress A, Saurer M, Frank D, Leuenberger M (2012) Methods to merge overlapping tree-ring isotope series to generate multi-centennial chronologies. *Chem Geol* 294:127–134
- Harris I, Jones PD, Osborn TJ, Lister DH (2014) Updated high-resolution grids of monthly climatic observations—the CRU TS3.10 dataset. *Int J Climatol* 34:623–642
- Hartl-Meier C, Zang C, Büntgen U, Esper J, Rothe A, Göttele A, Dirnböck T, Treydte K (2015) Uniform climate sensitivity in tree-ring stable isotopes across species and sites in a mid-latitude temperate forest. *Tree Phys* 35:4–15
- Heinrich I, Touchan R, Dorado Linan I, Vos H, Helle G (2013) Winter-to-spring temperature dynamics in Turkey derived from tree rings since AD 1125. *Clim Dyn* 41:1685–1701
- Helama S, Arppe L, Timonen M, Mielikäinen K, Oinonen M (2015) Age-related trends in subfossil tree-ring $\delta^{13}\text{C}$ data. *Chem Geol* 416:28–35
- Hilasvuori E, Berninger F, Sonninen E, Tuomenvirta H, Jungner H (2009) Stability of climate signal in carbon and oxygen isotope records and ring width from Scots pine (*Pinus sylvestris* L.) in Finland. *J Quat Sci* 24:469–480
- Holmes RL (1983) Computer-assisted quality control in tree-ring dating and measurement. *Tree-Ring Bull* 43:69–78
- Konter O, Holzkämper S, Helle G, Büntgen U, Saurer M, Esper J (2014) Climate sensitivity and parameter coherency in annually resolved $\delta^{13}\text{C}$ and $\delta^{18}\text{O}$ from *Pinus uncinata* tree-ring data in the Spanish Pyrenees. *Chem Geol* 377:12–19
- Kortelainen NM, Karhu JA (2004) Regional and seasonal trends in the oxygen and hydrogen isotope ratios of Finnish ground waters: a key for mean annual precipitation. *J Hydrol* 285:143–157
- Kress A, Saurer M, Büntgen U, Treydte KS, Bugmann H, Siegwolf TW (2009) Summer temperature dependency of larch budmoth outbreaks revealed by Alpine tree-ring isotope chronologies. *Oecologia* 160:353–365
- Kress A, Saurer M, Siegwolf RTW, Frank DC, Esper J, Bugmann H (2010) A 350 year drought reconstruction from Alpine tree-ring stable isotopes. *Glob Biogeo Cyc*. <https://doi.org/10.1029/2009GB003613>
- Labuhn I, Daux V, Girardclos O, Stievenard M, Pierre M, Masson-Delmotte V (2016) French summer droughts since 1326 CE: a reconstruction based on tree ring cellulose $\delta^{18}\text{O}$. *Clim Past* 12:1101–1117
- Leavitt SW (2010) Tree-ring C–H–O isotope variability and sampling. *Sci Tot Environ* 8:5244–5253
- Leavitt SW, Long A (1989) Drought indicated in carbon-13/carbon-12 ratios of southwestern tree rings. *Water Resour Bull* 25:341–347
- Linderholm HW, Björklund J, Seftigen K, Gunnarson BE, Fuentes M (2015) Fennoscandia revisited: a spatially improved tree-ring reconstruction of summer temperatures for the last 900 years. *Clim Dyn* 45:933–947
- Liu Y, Cai Q, Liu W, Yang Y, Sun J, Song H, Li X (2008) Monsoon precipitation variation recorded by tree-ring $\delta^{18}\text{O}$ in arid Northwest China since AD 1878. *Chem Geol* 252:56–61
- Loader NJ, Robertson I, McCarroll D (2003) Comparison of stable carbon isotope ratios in the whole wood, cellulose and lignin of oak tree-rings. *Palaeogeogr Palaeoclim Palaeoecol* 196:395–407
- Loader NJ, Young GHF, Grudd H, McCarroll D (2013) Stable carbon isotopes from Torneträsk, northern Sweden provide a millennial length reconstruction of summer sunshine and its relationship to Arctic circulation. *Quat Sci Rev* 62:97–113
- Luterbacher J, Xoplaki E, Dietrich D, Rickli R, Jacobeit J, Beck C, Gyalistras D, Schmutz C, Wanner H (2002) Reconstruction of sea level pressure fields over the Eastern North Atlantic and Europe back to 1500. *Clim Dyn* 18:545–561
- Luterbacher J et al (2016) European summer temperatures since Roman times. *Environ Res Lett*. <https://doi.org/10.1088/1748-9326/11/2/024001>
- Matalas NC (1962) Statistical properties of tree ring data. *Hydrol Sci J* 7:39–47
- Meko DM (1981) Applications of Box-Jenkins methods of time series analysis to the reconstruction of drought from tree rings. PhD Dissertation, Tucson
- Mischel M, Esper J, Keppeler F, Greule M, Werner W (2015) $\delta^2\text{H}$, $\delta^{13}\text{C}$ and $\delta^{18}\text{O}$ from whole wood, α -cellulose and lignin methoxyl groups in *Pinus sylvestris*: a multi-parameter approach. *Isotop Environ Health Stud* 51:553–568
- New M, Hulme M, Jones P (1999) Representing twentieth-century space–time climate variability. Part I: development of a 1961–90 mean monthly terrestrial climatology. *J Clim* 12:829–856
- New M, Lister D, Hulme M, Makin I (2002) A high-resolution data set of surface climate over global land areas. *Clim Res* 21:1–25
- Ododo JC, Agbakwuru JA, Ogbu FA (1996) Correlation of solar radiation with cloud cover and relative sunshine duration. *Energy Convers Manag* 37:1555–1559
- Porter TJ, Pisaric MF, Field RD, Kokelj SV, Edwards TW, Healy R, LeGrande AN (2014) Spring–summer temperatures since AD 1780 reconstructed from stable oxygen isotope ratios in white spruce tree-rings from the Mackenzie Delta, northwestern Canada. *Clim Dyn* 42:771–785
- Reddy SJ (1974) An empirical method for estimating sunshine from total cloud amount. *Sol Energy* 15:281–285
- Riechelmann DFC, Maus M, Dindorf W, Schöne B, Scholz D, Esper J (2014) Sensitivity of whole wood stable carbon and oxygen isotope values to milling procedures. *Rap Comm Mass Spectr* 28:1371–1375
- Riechelmann DFC, Maus M, Dindorf W, Konter O, Schöne B, Esper J (2016) Comparison of $\delta^{13}\text{C}$ and $\delta^{18}\text{O}$ from cellulose, whole wood, from an old high elevation *Pinus uncinata* in the Spanish Central Pyrenees. *Isotop Environ Health Stud*. <https://doi.org/10.1080/10256016.2016.1161622>
- Rinn F (2005) TSAP Win—time series analysis and presentation for dendrochronology and related applications. User reference, Heidelberg
- Rinne KT, Loader NJ, Switsur VR, Waterhouse JS (2013) 400-year May–August precipitation reconstruction for Southern England using oxygen isotopes in tree rings. *Quat Sci Rev* 60:13–25
- Roden JS, Ehleringer JR (1999) Observations of hydrogen and oxygen isotopes in leaf water confirm the Craig-Gordon model under wide-ranging environmental conditions. *Plant Physiol* 120:1165–1173
- Rozanski K, Araguas-Araguas L, Gonfiantini R (1992) Relation between long-term trends of oxygen-18 isotope composition of precipitation and climate. *Science* 258:981–985
- Saurer M, Siegenthaler U, Schweingruber F (1995) The climate-carbon isotope relationship in tree-rings and the significance of site conditions. *Tellus B* 47:320–330
- Saurer M, Siegwolf R, Schweingruber F (2004) Carbon isotope discrimination indicates improving water-use efficiency of trees in northern Eurasia over the last 100 years. *Glob Change Biol* 10:2109–2120
- Saurer M, Cherubini P, Reynolds-Henne CE, Treydte KS, Anderson WT, Siegwolf RTW (2008) An investigation of the common signal in tree ring stable isotope chronologies at temperate sites. *J Geophys Res*. <https://doi.org/10.1029/2008JG000689>
- Schleser GH, Anhof D, Helle G, Vos H (2015) A remarkable relationship of the stable carbon isotopic compositions of wood and cellulose in tree-rings of the tropical species *Cariniana micrantha* (Ducke) from Brazil. *Chem Geol* 401:59–66
- Schneider L, Smerdon J, Büntgen U, Wilson R, Myglan VS, Kirilyanov A, Esper J (2015) Revising midlatitude summer temperatures

- back to AD 600 based on a wood density network. *Geophys Res Lett.* <https://doi.org/10.1002/2015GL063956>
- Seftigen K, Linderholm HW, Loader NJ, Liu Y, Young GH (2011) The influence of climate on $^{13}\text{C}/^{12}\text{C}$ and $^{18}\text{O}/^{16}\text{O}$ ratios in tree ring cellulose of *Pinus sylvestris* L. growing in the central Scandinavian Mountains. *Chem Geol* 286:84–93
- Sidorova OV, Siegwolf RT, Saurer M, Naurzbaev MM, Vaganov EA (2008) Isotopic composition ($\delta^{13}\text{C}$, $\delta^{18}\text{O}$) in wood and cellulose of Siberian larch trees for early Medieval and recent periods. *J Geophys Res Biogeosci.* <https://doi.org/10.1029/2007JG000473>
- Stuiver M, Braziunas TF (1987) Tree cellulose $^{13}\text{C}/^{12}\text{C}$ isotope ratios and climatic change. *Nature* 328:58–60
- Tejedor E, Saz MA, Cuadrat JM, Esper J, de Luis M (2017) Summer drought reconstruction in Northeastern Spain inferred from a tree-ring latewood network since 1734. *Geophys Res Lett.* <https://doi.org/10.1002/2017GL074748>
- Treydte K, Schleser GH, Schweingruber FH, Winiger M (2001) The climatic significance of $\delta^{13}\text{C}$ in subalpine spruces (Lötschental/Swiss Alps)—a case study with respect to altitude, exposure and soil moisture. *Tellus B* 53:593–611
- Treydte K, Schleser GH, Helle G, Frank DC, Winiger M, Haug GH, Esper J (2006) The twentieth century was the wettest period in Northern Pakistan over the past millennium. *Nature* 440:1179–1182
- Treydte K et al (2007) Signal strength and climate calibration of a European tree ring isotope network. *Geophys Res Lett.* <https://doi.org/10.1029/2007GL031106>
- Treydte K, Frank DC, Saurer M, Helle G, Schleser G, Esper J (2009) Impact of climate and CO_2 on a millennium-long tree-ring carbon isotope record. *Geochim Cosmochim Acta* 73:4635–4647
- Treydte K, Boda S, Graf Pannatier E, Fonti P, Frank D, Ullrich B, Saurer M, Siegwolf R, Battipaglia G, Werner W, Gessler A (2014) Seasonal transfer of oxygen isotopes from precipitation and soil to the tree ring: source water versus needle water enrichment. *New Phytol* 202:772–783
- Trouet V, van Oldenborgh GJ (2013) KNMI climate explorer: a web-based research tool for high-resolution paleoclimatology. *Tree Ring Res* 69:1–13
- Trouet V, Esper J, Graham NE, Baker A, Scourse JD, Frank DC (2009) Persistent positive North Atlantic oscillation mode dominated the Medieval Climate Anomaly. *Science* 324:78–80
- Trouet V, Harley GL, Domínguez-Delmás M (2016) Shipwreck rates reveal Caribbean tropical cyclone response to past radiative forcing. *Proc Nat Acad Sci* 13:3169–3174
- van Oldenborgh GJ, Burgers G (2005) Searching for decadal variations in ENSO precipitation teleconnections. *Geophys Res Lett.* <https://doi.org/10.1029/2005GL023110>
- van der Schrier G, Briffa KR, Jones PD, Osborn TJ (2006) Summer moisture variability across Europe. *J Clim* 19:2818–2834
- Verheyden A, Roggeman M, Bouillon S, Elskens M, Beeckman H, Koedam N (2005) Comparison between $\delta^{13}\text{C}$ of α -cellulose and bulk wood in the mangrove tree *Rhizophora mucronata*: implications for dendrochemistry. *Chem Geol* 219:275–282
- von Storch H, Zorita E, Jones J, Dimitriev Y, Gonzalez-Rouco JF, Tett SFB (2004) Reconstructing past climate from noise data. *Science* 306:679–682
- Wanner H, Brönnimann S, Casty C, Gyalistras D, Luterbacher J, Schmutz C, Stephenson DB, Xoplaki E (2001) North Atlantic oscillation—concepts and studies. *Surveys Geophys* 22:321–381
- Waterhouse JS, Barker AC, Carter AHC, Agafonov LI, Loader NJ (2000) Stable carbon isotopes in Scots pine tree rings preserve a record of flow of the river Ob. *Geophys Res Lett* 27:3529–3532
- Weigt RB et al (2015) Comparison of $\delta^{13}\text{C}$ and $\delta^{18}\text{O}$ values between tree-ring whole wood and cellulose in five species growing under two different site conditions. *Rapid Commun Mass Spectr* 29:2233–2244
- Wilson AT, Grinsted MJ (1977) $^{12}\text{C}/^{13}\text{C}$ in cellulose and lignin as palaeothermometers. *Nature* 265:133
- Wilson RJS et al (2016) Last millennium Northern Hemisphere summer temperatures from tree rings. Part I: the long term context. *Quat Sci Rev* 134:1–18
- Zeng X, Liu X, Treydte K, Evans MN, Wang W, An W, Sun W, Xu G, Wu G, Zhang X (2017) Climate signals in tree-ring $\delta^{18}\text{O}$ and $\delta^{13}\text{C}$ from southeastern Tibet: insights from observations and forward modelling of intra- to interdecadal variability. *New Phytol.* <https://doi.org/10.1111/nph.14750>